Chemosphere 393 (2025) 144759

Contents lists available at ScienceDirect

Chemosphere

journal homepage: www.elsevier.com/locate/chemosphere

Soluble extracellular polymeric substances and microplastics: Exposure-response and circular reuse for removal

Filipa Rodrigues [a,b,c], Ivana Mendonça [a,b,c], Marisa Faria [a,b], Ricardo Gomes [a], Juan L. Gómez Pinchetti [d], Artur Ferreira [c], Nereida Cordeiro [a,b,*]

[a] LB3, Faculty of Science and Engineering, University of Madeira, 9020-105, Funchal, Portugal
[b] CIIMAR, Interdisciplinary Centre of Marine and Environmental Research, University of Porto, 4450-208, Matosinhos, Portugal
[c] CICECO, Aveiro Institute of Materials and Águeda School of Technology and Management, University of Aveiro, 3754-909, Águeda, Portugal
[d] Spanish Bank of Algae, Institute of Oceanography and Global Change (IOCAG), University of Las Palmas de G.C, Muelle de Taliarte S/N, Telde, Canary Islands, 35214, Las Palmas, Spain

HIGHLIGHTS

- Circular reuse: S-EPS pre-treat micro-algal-intake seawater with MPs.
- PS-MP exposure stimulates S-EPS, up to 34%.
- RSM optimised S-EPS to 113 mg/L in 7 days.
- 82% PS-MP removal (Fe^{3+} 0.05%, pH 3.5; 60 min).
- Mechanism: charge neutralisation/ bridging.

GRAPHICAL ABSTRACT

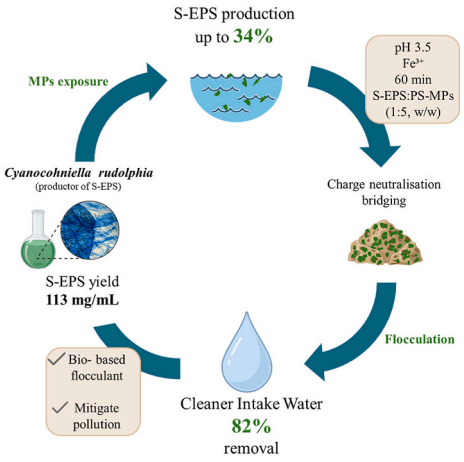

ARTICLE INFO

Handling editor: Dr A ADALBERTO NOYOLA

Keywords:
Cyanocohniella rudolphia
Soluble extracellular polymeric substances
Microplastics
Polystyrene
Bioflocculation
Circular economy

ABSTRACT

Microplastics (MPs) are pervasive in aquatic systems, threatening ecosystems, human health, and microalgal production. Soluble extracellular polymeric substances (S-EPS) can agglomerate particles and aid removal. This study examines S-EPS from the cyanobacterium *Cyanocohniella rudolphia* (BEA 0786B) to *(i)* model and optimise S-EPS production, *(ii)* assess production in water contaminated with polystyrene MPs (PS-MPs), and *(iii)* test S-EPS as a bioflocculant for PS-MPs removal. Response surface methodology (RSM) defined a cost-lean operating window and predicted an optimum S-EPS titre of 113 mg/L at 7 days using 10 g/L nitrogen, 0.98 g/L phosphorus, and a biomass-to-medium ratio of 1:6.87 (w/v). Cultures were challenged with PS-MPs (50 μg/L and 5 mg/L) under static or aerated conditions, and at both exponential and stationary phases, and showed stimulated S-EPS synthesis with increases of up to 34%, depending on hydrodynamics and growth stage. Purified S-EPS were

* Corresponding author. LB3, Faculty of Science and Engineering, University of Madeira, 9020-105, Funchal, Portugal.
E-mail address: ncordeiro@staff.uma.pt (N. Cordeiro).

https://doi.org/10.1016/j.chemosphere.2025.144759
Received 12 September 2025; Received in revised form 5 November 2025; Accepted 6 November 2025
Available online 12 November 2025

evaluated as a bioflocculant at 2 g/L PS-MPs to probe robustness and rate-limiting mechanisms and to delineate a conservative operating window. Maximum removal of 82% was achieved in freshwater at pH 3.5 with Fe^{3+} 0.05% (w/w), 25 °C, S-EPS dose 400 mg/L (S-EPS:PS-MPs 1:5, w/w), and 60 min flocculation. Zeta potential trends and microscopy support charge neutralisation/bridging as the dominant mechanism. Compatible with standard coagulation/flocculation units, the approach links cost-lean, cultivation-derived S-EPS (typically discarded) to their reuse as a low-additive pretreatment for algal-cultivation intake waters (freshwater/low-salinity), reducing reliance on synthetic coagulants and added salinity/metal-sludge burdens. Overall, *C. rudolphia* is a promising S-EPS producer, whose production is enhanced by exposure to PS-MPs, and its S-EPS acts as an efficient, bio-based flocculant for PS-MPs. The results support process designs to safeguard microalgal operations and to mitigate microplastic pollution in water. This work integrates RSM-optimised S-EPS production, environmental-level exposure-response, and a high-load removal benchmark, enabling circular, low-additive, drop-in pretreatment compatible with standard coagulation/flocculation units.

1. Introduction

Microplastic (MP) pollution in aquatic environments is pervasive and escalating, demanding solutions that are both effective and sustainable. Often invisible to the naked eye, MPs represent a persistent and emerging threat to aquatic ecosystems and human health (Revel et al., 2018; Rist et al., 2018; Yuan et al., 2022). MPs arise either as secondary particles from the fragmentation of larger plastics via physical, chemical, or biological processes, or as primary particles intentionally manufactured for consumer products (Esmaeili Nasrabadi et al., 2025a, 2025b). Their small size (<5 mm) and persistence hinder conventional water treatment, enabling infiltration into natural ecosystems (Wagner and Lambert, 2018; Elizalde-Velázquez and Gómez-Oliván, 2021; Ding et al., 2021; Sarijan et al., 2021; Mendonça et al., 2024). Human exposure occurs via ingestion (drinking water, seafood, table salt), inhalation of airborne fibres/particles, and, less prominently, dermal contact. Reported toxicological pathways in mammalian and cellular models include oxidative stress, inflammatory responses, epithelial/barrier disruption, and endocrine-active effects; outcomes depend on particle size, surface chemistry, and co-adsorbed contaminants. Evidence for tissue translocation has been reported, although dose–response relationships at environmental concentrations remain under investigation (Xie et al., 2020; Zhao et al., 2024).

MPs bioaccumulate across taxa, from zooplankton and filter-feeding bivalves to fish and seabirds, and trophic transfer along food webs has been documented, with consequences for energy budgets and the condition of predators. At the ecosystem level, exposure can reduce feeding and fecundity in plankton and bivalves, alter grazing/filtration rates and the size structure of planktonic communities, and modify benthic processes; deposition in sediments creates a long-term sink with episodic resuspension. Their high surface-to-mass ratios and surface roughness enable adsorption and transport of dissolved pollutants (*e.g.,* metals, hydrophobic organics), and weathering/aging and biofilm formation further enhance these vector effects. These outcomes depend on particle size/shape, polymer type and weathering, and on water chemistry (*e.g.*, salinity and organic matter) (Barnes et al., 2009; Cole et al., 2015; Wagner and Lambert, 2018; Elizalde-Velázquez and Gómez-Oliván, 2021; Ding et al., 2021; Ebrahimi et al., 2022; Jiménez-Skrzypek et al., 2021; Mendonça et al., 2024).

In aquatic systems, prevalent polymers include polyethylene (PE; LDPE/HDPE), polypropylene (PP), polystyrene (PS), polyvinyl chloride (PVC), polyethylene terephthalate (PET), and polyamides (PA). Typical particle shapes are fibres, fragments, films, beads, and foams. Differences in surface chemistry (hydrophobicity/functional groups) and density govern transport, partitioning, and amenability to charge-mediated flocculation. Hydrophobic MPs typically bear a negative ζ-potential near circumneutral pH, a feature relevant to flocculation by acidic soluble extracellular polysaccharides. Within this mechanistic context, PS is widely used as a representative hydrophobic MP because it combines defined surface chemistry, stable electrokinetic behaviour, and narrow size distributions that facilitate reproducible dispersion, imaging, and mass-normalised removal metrics. PS is also frequently reported in environmental surveys and has been documented to have biological effects, including impacts on marine organisms and relevance to algal-cultivation intake waters (Barnes et al., 2009; Cole et al., 2015; Wang et al., 2019; Cunha et al., 2020a; Mendonça et al., 2023a). MP contamination increasingly affects intake waters used in algal bioprocessing, with potential impacts on productivity and product quality; practical, low-additive mitigation strategies remain limited. Cyanobacteria produce extracellular polymeric substances (EPS) with physicochemical properties that can promote MP aggregation and removal, offering a bio-based route compatible with sustainable processes (Cunha et al., 2019, 2020b). EPS occur at different cellular levels and are commonly classified into two categories: bound EPS (B-EPS), including sheaths, capsular polymers, transparent condensed gels, loosely attached polymers, and adhered organic material, and soluble EPS (S-EPS), comprising soluble macromolecules, colloids, and slimes (Camacho-Chab et al., 2016; Franco-Morgado et al., 2023). EPS play pivotal roles in biofilm formation, nutrient cycling, and cellular protection (Costa et al., 2018). Their adsorption capacity, biodegradability, and ability to form bridging structures support their use as bio-based flocculants for MP removal (Xiao and Zheng, 2016; Cunha et al., 2019, 2020b; Siddharth et al., 2021; Feng et al., 2021; Faria et al., 2022; Mendonça et al., 2023b; Rodrigues et al., 2024b). In this context, S-EPS, being dissolved or colloidal, are particularly attractive because they can rapidly mediate collision–attachment with hydrophobic MPs via charge neutralisation and polymer bridging. However, links between exposure–response, operating windows for removal, and process-level reuse of cultivation-derived S-EPS remain insufficiently established. The present study maps exposure effects on S-EPS production and defines removal performance under controlled conditions, providing an operational basis for circular, low-additive pretreatment of MP-contaminated waters.

From a cleaner production and circular economy perspective, leveraging photosynthetically derived EPS couples pollutant mitigation with renewable biopolymer generation (CO_2 capture, low inputs). The utilisation of EPS for capturing and removing MPs not only addresses MP pollution but also contributes to circularity by valorising culture by-products as functional materials, thereby promoting sustainable industrial practices. Here, S-EPS recovered from cultivation are positioned as an in-process flocculant for intake waters, closing the loop between production and application. This coupling reduces reliance on synthetic coagulants and aligns with low-input, photosynthetic manufacturing.

To fully recognise the potential of cyanobacteria-based EPS and maximise its value, production must be increased under cost-effective conditions and linked to application performance. Various physicochemical parameters, light intensity, temperature, nutrient availability and carbon source affect EPS production in cyanobacteria (Tiwari et al., 2015; Cruz et al., 2020). Response surface methodology (RSM) provides a statistically rigorous framework to quantify factor interactions and locate operating optima for S-EPS synthesis. RSM enables construction of mathematical models between selected factors (*e.g.,* temperature, nutrient concentrations and cultivation time) and responses (S-EPS titre or biomass), supporting prediction and optimisation (Trabelsi et al.,

2009; Asgher et al., 2020; Borah et al., 2020; Zhao et al., 2020; Ahmed et al., 2023). However, explicit coupling of RSM-optimised S-EPS production with *(i)* production responses under realistic MP-contamination scenarios and *(ii)* systematic performance maps for MP removal across relevant water chemistries remains scarce.

This study examines the cyanobacterium *Cyanocohniella rudolphia* with three objectives: *(i)* to develop and validate an RSM model for forecasting and optimising S-EPS production; *(ii)* to quantify the effect of exposure to polystyrene microplastics (PS-MPs) on S-EPS production and biomass across growth phases (exponential *vs*. stationary) and hydrodynamic regimes (with *vs*. without aeration); and *(iii)* to evaluate purified S-EPS as a bioflocculant for PS-MPs, and to identify the dominant removal mechanisms. By explicitly linking production optimisation to application performance, the study advances a cleaner production route that can be integrated into microalgal operations and water treatment within a circular economy framework.

2. Materials and methods

2.1. Strain and culture conditions

C. rudolphia (BEA 0786B) was isolated from a hypersaline environment in Spain (Añana Saltworks, Álava) and obtained from the Spanish Bank of Algae (BEA). *C. rudolphia* was grown in Spirulina medium (Electronic Supplementary (ES) - ES1), with an irradiance of 40 μmol photons m^{-2} s^{-1}, a 14:10 h (light: dark) photoperiod (Aralab CP500 growth chamber), and 22 ± 1 °C, until stationary phase (OD_{750} = 1.08, corresponding to 1.286 ± 0.311 g/L; biomass dry weight per culture volume) was reached. Due to frequent aggregation into colonies or filaments, biomass dry weight was used as the primary growth metric rather than individual cell counts. Aseptically collected aliquots from the homogeneous culture were used to monitor S-EPS and biomass throughout the experiments. Samples were centrifuged (HERMLE Z360) at 4427 *xg* for 10 min. The supernatant was used to quantify S-EPS released to the medium, while the pellet was dried at 40 °C to a constant mass to determine *C. rudolphia* biomass.

2.2. Preparation and characterisation of PS-MPs

Polystyrene microplastics (PS-MPs), used here as a model hydrophobic MP commonly detected in aquatic environments, were prepared from a commercial blue polystyrene granulate (UV-Granulate; Magical Pyramid Bruecher & Partner KG). The material was ground using a milling machine (230 V, 50 Hz, 120 W) to obtain a size fraction <100 μm. Following grinding and fractionation, the PS-MPs were washed with *n*-hexane (analytical grade; PanReac AppliChem/ITW Reagents) to remove surface contaminants, filtered through a sintered-glass G4 crucible (nominal pore size 10–16 μm, VWR) to collect the <16 μm fraction, dried at 60 °C overnight and stored in a desiccator until use. Two stock dispersions were prepared in culture medium containing 0.1% (v/v) Tween 20 (polysorbate 20; Sigma-Aldrich), which was kept constant across all assays and controls to aid dispersion, at 50 μg/L (environmental level) and 5 mg/L (high level). A blank dispersion (PS-MPs with Tween 20, without S-EPS, and without added cation) was included to control for dispersant effects. The surface charge of PS-MPs was determined by zeta potential measurements (see Section 2.8). Unless stated otherwise, reagents were analytical grade and used as received; water was bidistilled (2.7 μS/cm).

2.3. Experimental design and RSM modelling

To quantify the influence of abiotic factors on S-EPS and biomass, an initial screening defined workable factor ranges using a one-factor-at-a-time (OFAT) approach (Mehra and Jutur, 2022). The factors examined were: *(i)* the culture-medium volume to wet-biomass mass ratio, R (1:1 to 14:1; mL/g); *(ii)* production cycle duration, D (1–7 days); *(iii)* phosphorus concentration, P (0.5–2.0 g/L); and *(iv)* nitrogen concentration, N (2.5–10.0 g/L). S-EPS titre and biomass concentration were treated as response variables.

After screening, RSM was implemented in Design-Expert (version 13) using a face-centred central composite design (CCD; α = 1). P was excluded from the CCD due to negligible effect in the screening, while R, D, and N were retained within the same ranges (R: 1:1–14:1 mL/g; D: 1–7 days; N: 2.5–10.0 g/L). The complete design specification and statistical validation (design size, star/factorial/centre points, ANOVA, lack-of-fit, residual diagnostics, and R^2 metrics) are described in Rodrigues et al. (2024a), using *C. rudolphia* as the case study. All experiments were conducted in triplicate, and analysis of variance (ANOVA) was used to assess model significance and adequacy.

S-EPS released to the medium was quantified by the Alcian Blue binding assay (see ES2). The method was validated for linearity, sensitivity, and matrix effects; details are summarised in ES2 and will be presented in full elsewhere (Rodrigues et al., 2025). A calibration curve (Fig. S1) was constructed using purified S-EPS obtained from an axenic *C. rudolphia* culture (Section 2.5).

2.4. Exposure of cultures to PS-MPs

To evaluate the effect of polystyrene microplastics (PS-MPs) on S-EPS production by *C. rudolphia*, the biomass-to-medium ratio (R) was fixed at 1:12.5 (w/v; g/mL; equivalent to R = 12.5 mL/g). Cultures were grown in medium containing two PS-MPs concentrations, 50 μg/L (environmental) and 5 mg/L (high), under two hydrodynamic regimes: static culture (SC) and aerated culture (AF), and at two growth states: exponential (exp) and stationary (sta). AF received sterile air from an N-ACO 60 pump (AquaNova) through 0.22 μm PTFE (Sartorius) inline filtration and was sparged directly into the liquid via a sterile glass Pasteur pipette used as the air outlet (tip inner diameter of 0.8 mm). The airflow was set to 0.30 vvm (litres of air per minute per litre of liquid), generating fine bubbles and bubble-induced circulation without mechanical stirring. SC had no forced mixing. Experiments lasted 7 days, initiated at OD_{750} = 0.75 for exponential-phase inoculum (0.926 ± 0.019 g/L, dry weight) and OD_{750} = 1.08 for stationary-phase inoculum (1.286 ± 0.311 g/L, dry weight). At each sampling point, S-EPS and biomass were isolated and quantified as described in Section 2.1. To assess the impact of PS-MPs on medium rheology, culture supernatants were used for viscosity measurements (see ES3). Cell morphology and S-EPS distribution were examined by optical microscopy after Alcian Blue staining (see ES2).

2.5. S-EPS isolation and characterisation

To isolate the S-EPS, culture supernatants obtained after centrifugation of the biomass (see Section 2.1) were processed by tangential-flow ultrafiltration (Vivaflow 50R). In this process, the supernatant was circulated across a membrane with a 100 kDa molecular-weight cut-off (MWCO), Hydrosart (regenerated cellulose); effective membrane area: 50 cm^2; operated at a transmembrane pressure of 2.5 bar and a cross-flow rate of 300 mL/min, retaining macromolecular S-EPS while removing low-molecular-mass solutes and salts. A diafiltration protocol comprising 12 consecutive concentration–dilution cycles (2.5 times the retentate volume per cycle) with bidistilled water was applied to ensure thorough purification (Fig. S2). This process was continued until conductivity stabilised at 2.7 μS/cm (Consort C5020). Viscosity was measured at multiple temperatures on S-EPS-containing supernatants (pre-ultrafiltration) and on ultrafiltration retentates (post-purification) to assess the influence of salt ions on rheological behaviour (see ES3; Fig. S3). The purified S-EPS was then characterised by Attenuated total reflection-Fourier transform infrared spectroscopy (ATR-FTIR; 4 cm^{-1} resolution, 32–64 scans), ^{1}H NMR spectroscopy (Bruker Avance III 300 MHz, D_2O, 70 °C, 1000 scans, water suppression zgespg), scanning electron microscopy (SEM; Hitachi SU-70 HR-FESEM; carbon coating

Emitech K950X) and ζ-potential measurements (Zetasizer Nano ZSP, 25 °C; Smoluchowski model) (details in Sections 2.7-2.8 and ES4-ES5).

2.6. Jar-test bioflocculation assays

The bioflocculant potential of *C. rudolphia*-based S-EPS was assessed in jar-test assays at 25 ± 2 °C. Assays emulate pretreatment of microalgal-cultivation intake seawater to map a low-additive operating window. Unless otherwise stated, a volumetric mixing ratio of 46.5:2.5:1 (PS-MPs dispersion: cation solution: S-EPS solution) was used. Assays were performed in bidistilled water (2.7 μS/cm), and pH was adjusted with HCl (1 M) or NaOH (1 M) (analytical grade, VWR Chemicals). Briefly, the PS-MPs dispersion and the selected cation solution were premixed at 700 rpm for 5 min on a magnetic stirrer; the S-EPS solution was then added, and the mixture was stirred at 100 rpm for 60 min. After mixing, samples were allowed to settle for the specified settling time, and 1 mL was withdrawn from the mid-depth of the supernatant. All assays were performed in triplicate (n = 3). Turbidity of the collected samples was measured at 750 nm (OD_{750}) in a quartz cuvette (1 cm path length) using a UV-6300PC double-beam spectrophotometer. The bioflocculation rate (%) was calculated using Eq. (1), where OD_{750b} and OD_{750s} represent the absorbance of the blank (PS-MPs dispersion without S-EPS or added cation) and the sample, respectively.

$$\textit{Bioflocculation}\ \text{rate}\ (\%) = \frac{OD_{750b} - OD_{750s}}{OD_{750s}} * 100 \quad (1)$$

Physicochemical parameters representative of contaminated waters were varied as follows: cation type (Fe^{3+} as $FeCl_3.6H_2O$, Ca^{2+} as $CaCl_2$, Mg^{2+} as $MgCl_2.4H_2O$, all analytical grade (VWR Chemicals, Belgium; each at 0.448 mM); Fe^{3+} concentration 0.03–0.95% (w/w); pH (3–7); salinity (0–37 ‰, adjusted with NaCl, analytical grade; VWR Chemicals, Belgium); S-EPS:PS-MPs mass ratios (1:5, 1:50, 1:500); and settling time (30, 60, 120 min). To elucidate interaction mechanisms between S-EPS and PS-MPs, hetero-aggregates were examined by optical and fluorescence microscopy (see ES2), and surface charge was quantified by zeta-potential measurements (see Section 2.8).

2.7. Microscopy characterisation

2.7.1. Scanning electron microscopy analysis

C. rudolphia cultures were prepared for SEM as follows. Samples were fixed in 2.5% (w/v) glutaraldehyde (EM-grade; Electron Microscopy Sciences) in phosphate buffer (0.1 mol/L, pH 7.2) at 4 °C overnight. After fixation, samples were rinsed twice with the same buffer (VWR Chemicals) and dehydrated through a graded ethanol (analytical grade; VWR Chemicals) series (30, 50, 70, 90, and 100% v/v; 10 min per step at room temperature, 23 ± 2 °C). Dehydrated material was freeze-dried and stored in a desiccator until imaging. Dried samples were mounted on metal stubs (adhesive carbon tape) and carbon-coated using an Emitech K950X turbo evaporator to ensure surface conductivity. Micrographs were acquired on a Hitachi SU-70 HR-FESEM operated at 4 kV (secondary-electron detection).

2.7.2. Bright-field and fluorescence microscopy

The characterisation of *C. rudolphia* cells was performed using both bright-field and epifluorescence microscopy on a Leica DM2700 P microscope equipped with a Leica DFC450C digital camera and a CoolLED pE-300 lite illumination system. Observations were conducted at 10x and 40x magnifications. Fluorescent signals corresponding to natural chlorophyll autofluorescence within the microalgal cells were detected using the I3 excitation/emission filter set (450–490 nm/515–565 nm), enabling visualisation of cell morphology.

2.8. Zeta potential measurements

Zeta potential of the individual matrices (S-EPS and PS-MPs) and of S-EPS/PS-MPs hetero-aggregates was measured using a Zetasizer Nano ZSP (Malvern Panalytical) with disposable folded-capillary cells. Measurements were performed at 25 °C and pH 7, after dilution with deionised water (Milli-Q). Data acquisition and processing were performed using the manufacturer's software (version 3.30). For each condition, three independent samples were prepared, each measured in triplicate (n = 3 × 3); samples were equilibrated in the cell for 120 s before measurement. Electrophoretic mobility was converted to Zeta potential using the Smoluchowski model, and results are reported as mean ± standard deviation.

2.9. Data and statistical analysis

Data analysis for response surface modelling and model ANOVA was performed in Design-Expert (version 13), and data handling/plotting in GraphPad Prism (version 9). For comparisons outside the design of experiments (DoE), one-way ANOVA was used to assess differences in cyanobacterial growth, S-EPS production under PS-MPs exposure, and PS-MPs removal by *C. rudolphia* S-EPS, with Tukey's HSD post hoc when multiple groups were compared. Assumptions of normality (Shapiro-Wilk) and homoscedasticity (Levene) were tested. When assumptions were violated, Welch's ANOVA with Games-Howell post hoc or, if needed, Kruskal-Wallis with Dunn-Bonferroni correction was used. Statistical significance was set at α = 0.05. Unless otherwise indicated, results are reported as mean ± SD from at least three biological replicates (n ≥ 3). Model-adequacy metrics for RSM are reported with the models (Rodrigues et al., 2024a).

3. Results and discussion

3.1. Optimisation and modelling of S-EPS production from C. rudolphia using RSM

Cyanobacteria require nitrogen (N) and phosphorus (P) for growth and metabolite synthesis (Liberton et al., 2022). To maximise S-EPS production by *C. rudolphia*, RSM was applied following an OFAT screening of four factors: biomass-to-medium ratio (R), production time (D), and P and N concentrations. The full central composite design (face-centred, α = 1), model diagnostics, and ANOVA are reported in Rodrigues et al. (2024a). Experimental verification of the RSM-predicted optimum (113.2 mg/L), including diagnostics for lack of fit and residuals, is also reported there. P showed an effect in screening and was held at 0.98 g/L for optimisation, while R (mL/g; mL medium per g wet biomass), D (days), and N (g/L) entered the final quadratic model. In coded variables, S-EPS production (Y, mg/L) was fitted by the second-order equation (Eq. (2)):

$$Y = 142.34 - 39.85R + 13.46D + 13.31N + 25.24R*D + 7.62R*N + 23.41R*R^2 \quad (2)$$

Model terms were significant by ANOVA, with R exerting the largest (negative) main effect (Pareto, Fig. S4), while D and N were positive. Interaction terms R × D and R × N were also positive, indicating that the adverse effect of high R (*i.e.,* dilute biomass) is mitigated at longer production times and higher N. Response surfaces (Fig. 1A and B) show that increasing R from 1 to 14 mL/g reduces S-EPS, consistent with N availability sustaining S-EPS biosynthesis in dilute cultures.

Two operating windows were derived. Under a cost-constrained objective (low biomass dilution), the optimum was R = 6.87 mL/g, D = 7 days, P = 0.98 g/L, N = 10 g/L, yielding a predicted S-EPS of 113.2 mg/L. Under a yield-maximising objective (no cost constraint), the optimum shifted to R = 1 mL/g, D = 1 day, P = 0.98 g/L, N = 10 g/L, with a predicted 223.1 mg/L. The first window is more compatible with cleaner-production goals (lower medium use per biomass), while the second illustrates the model's upper bound for S-EPS titres.

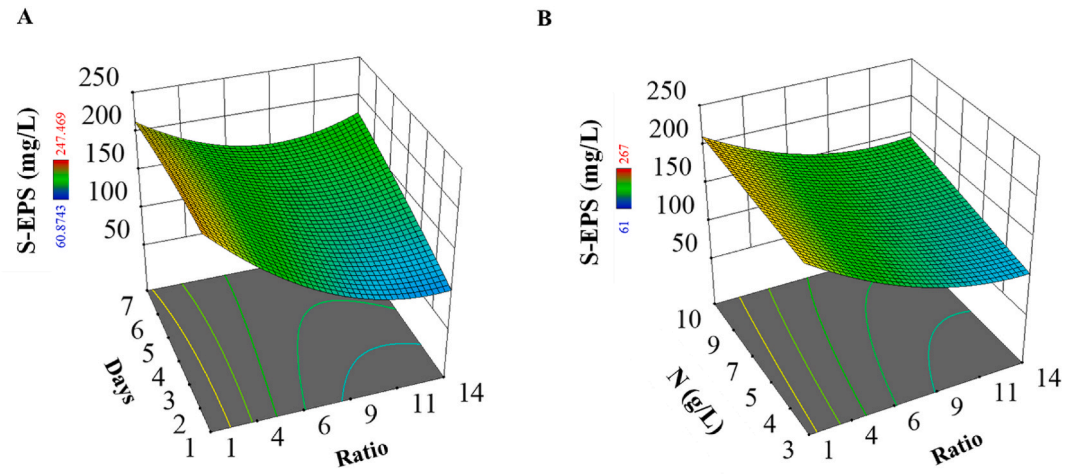

Fig. 1. Three-dimensional response-surface plots of S-EPS production. (**A**) Biomass-to-medium ratio (R, mL/g) *vs.* culture time (D, days) at fixed nitrogen (N = 6.25 g/L). (**B**) R (mL/g) vs. nitrogen (N, g/L) at fixed culture time (D = 4 days).

3.2. Impact of PS-MPs-contaminated water on S-EPS production

The effect of PS-MPs (50 μg/L and 5 mg/L) on S-EPS production by *C. rudolphia* was evaluated across growth phases (exponential, stationary) and hydrodynamic regimes (static, SC; aerated, AF). PS was used as the representative hydrophobic MPs (see Introduction). Apparent viscosity of culture supernatants at 25 °C (mPa·s) was used as an operational proxy for dissolved/colloidal S-EPS (ES3), and S-EPS yields were quantified on day 7. At 5 mg/L PS-MPs, viscosity trajectories over 7 days showed modest dependence on hydrodynamics and growth phase (Fig. 2). Two-way ANOVA (phase × hydrodynamics) indicated no significant interaction at most time points (Table S1); a single significant effect was detected on day 4 ($p < 0.05$). In AF, viscosity decreased transiently at days 2–3 and then increased to 14–17 mPa s by day 7 (from 9 to 10 mPa s at the early minimum). In SC, viscosity decreased on day 1 and then increased to 10–11 mPa s by day 7.

After 7 days, PS-MPs stimulated S-EPS relative to uncontaminated controls, with a concentration-dependent effect (50 μg/L < 5 mg/L) in most regimes (Fig. 3A; Table S1). A notable exception was AF-exp, where S-EPS did not differ significantly between the two PS-MPs concentrations. The radar-plot comparison versus matched controls (Fig. 3B) delineates two response regimes: *(i)* the most significant deviations from control occur in SC-sta cultures; *(ii)* more minor deviations occur in AF-exp cultures. Overall, the data indicate a stress-responsive increase in S-EPS that is amplified in the stationary phase, consistent with EPS up-regulation under stress (Sheikh et al., 2022), and attenuated under aeration during exponential growth, when resources are channelled to biomass formation. Similar PS-MP-induced S-EPS increases have been reported for *Chlorella vulgaris* and *Chlamydomonas reinhardtii* (Li et al., 2020; Demir-Yilmaz et al., 2022).

Biomass was largely unaffected by PS-MPs across phases and hydrodynamics (Fig. S5; Table S2), with a difference detected only at day 7 under AF; as expected, AF produced higher biomass than SC overall. The combination of maintained biomass and elevated S-EPS, particularly in SC–sta, identifies an operational niche aligned with cost-lean production while leveraging PS-MPs-triggered S-EPS secretion (Cunha et al., 2020a; Mendonça et al., 2023a). By contrast, AF-exp supports rapid biomass accumulation with smaller S-EPS perturbations, which suits throughput-oriented operations.

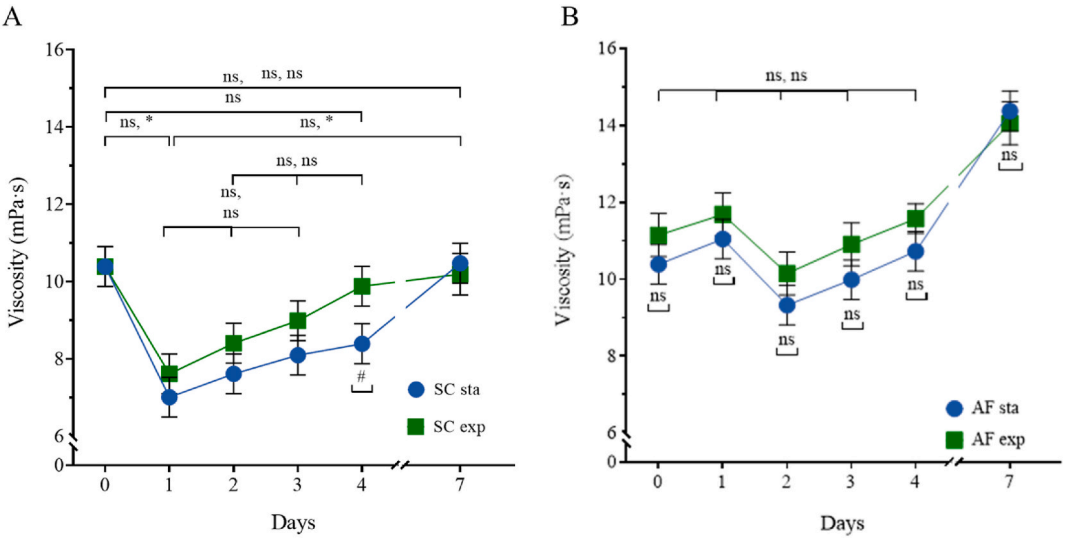

Fig. 2. Apparent viscosity over 7 days in PS-MPs–contaminated water (5 mg/L). (**A**) Static (SC) and (**B**) aerated (AF) production conditions under stationary (sta) and exponential (exp) growth phases, measurements at 25 °C with a Brookfield DV-III Ultra viscometer (spindle 02 at 100 rpm). Viscosity is used as an operational proxy for dissolved/colloidal S-EPS (ES3). Points/lines show mean ± SD (n = 3). Significance: * within-day differences; # differences between phases ($p < 0.05$); ns, not significant.

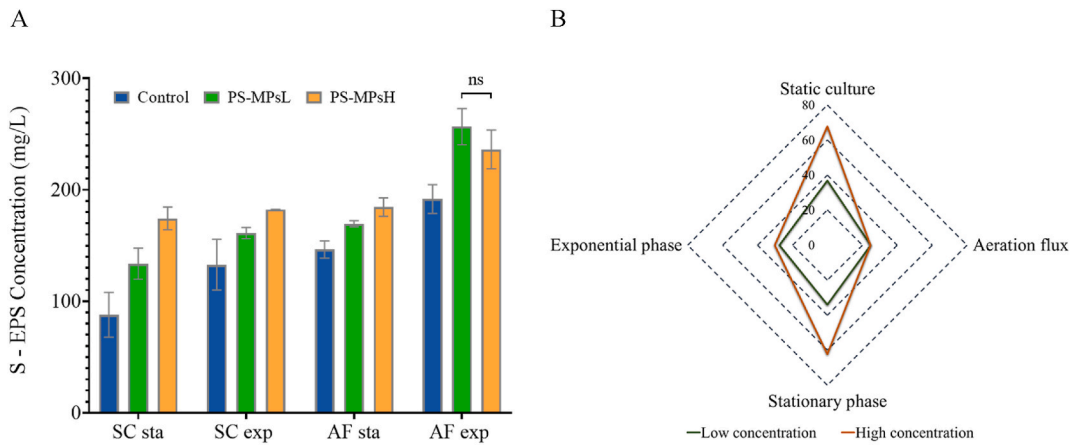

Fig. 3. Effects of PS-MPs-contaminated water on *C. rudolphia* S-EPS production after 7 days: (**A**) S-EPS yield (mg/L); (**B**) radar plot of the variation in S-EPS production relative to the control (exponential and stationary phase *C. rudolphia* in uncontaminated water). Static (SC) and aerated (AF) production; stationary (sta) and exponential (exp) phases; low (PS-MPsL; 50 μg/L) and high (PS-MPsH; 5 mg/L) contamination. ns - non-significant differences ($p \geq 0.05$).

3.3. Applying C. rudolphia-based S-EPS as a bioflocculant for PS-MPs removal

Microbially derived S-EPS are increasingly explored as sustainable bioflocculants (Tawila et al., 2018; Agunbiade et al., 2022; Mendonça et al., 2023b). Given the strong S-EPS secretion by cyanobacteria, *C. rudolphia* S-EPS was evaluated as a bio-based aid to remove PS-MPs from waters relevant to microalgal production. The focus was on how S-EPS structure and physicochemical context (cation type/-concentration, pH, salinity, S-EPS:PS-MPs ratio, and settling time) influence removal efficiency.

3.3.1. S-EPS characterisation

C. rudolphia exhibits life-cycle morphological plasticity, including *Nodularia*-like straight to slightly curved trichomes and a *Nostoc*-like stage with shorter, curved trichomes within a common sheath (Jung et al., 2022). Bright-field imaging confirmed the presence of typical trichomes (Fig. 4A) and revealed extensive Alcian Blue-positive reticulated matrices, consistent with S-EPS networks (Fig. 4B and C). SEM revealed a dense, fibrillar extracellular matrix consistent with a polysaccharidic-rich material (Fig. 4D). Under PS-MPs exposure, fluorescence microscopy showed that PS-MPs were retained within the S-EPS network (Fig. 4E), supporting a capture/bridging mechanism.

S-EPS was isolated from culture supernatants and purified by ultrafiltration (see Section 2.5), yielding a salt-depleted, particle-free material suitable for characterisation and flocculation tests (Fig. 4F). ATR-FTIR spectra showed broad O–H stretching around 3400 cm^{-1}, C–H stretching near 2920 cm^{-1}, and a carbohydrate fingerprint dominated by C–O–C/C–O vibrations in 1140-950 cm^{-1}, consistent with polysaccharides (ES4; Fig. S6) (Xu et al., 2013; Kaplan Can et al., 2019). A band at 1650 cm^{-1} is attributed to amide I and/or δ(H_2O), while amide II is weak/overlapped near 1550 cm^{-1}, consistent with minor protein; the feature at 1420 cm^{-1} is consistent with stretching vibration of the carboxylate group (COO^-) (Nobrega et al., 2019). Complementary ^1H

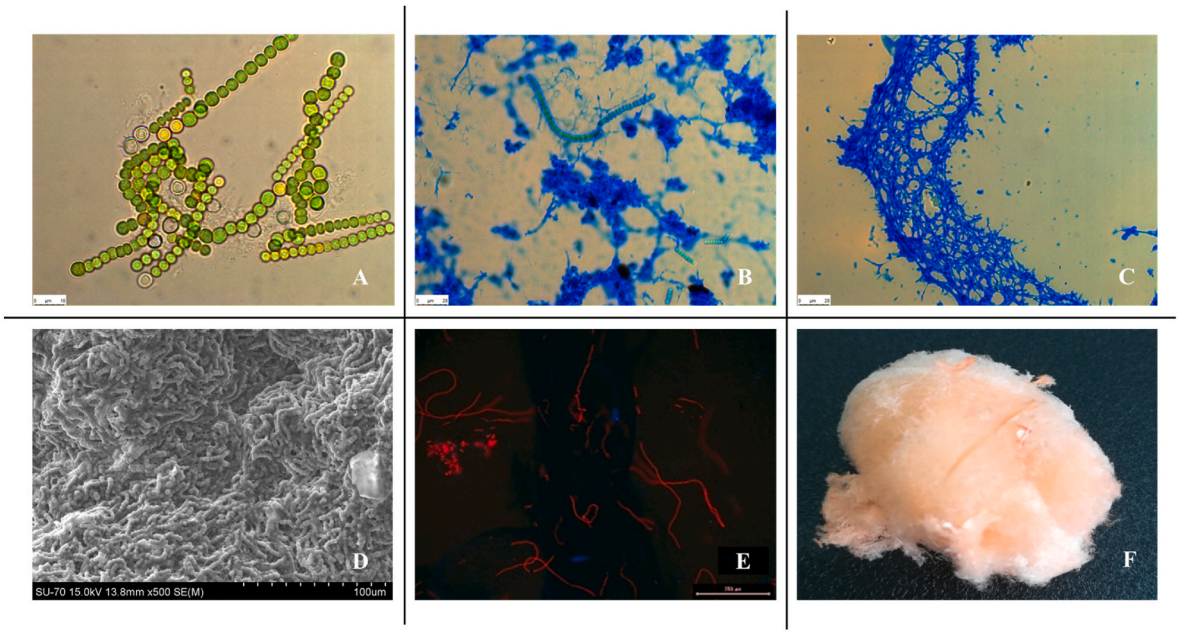

Fig. 4. Representative images supporting the bioflocculant role of *C. rudolphia* S-EPS. **(A)** Bright-field micrographs of *C. rudolphia* cells (40x). (**B**) *C. rudolphia* Culture medium with Alcian Blue-positive S-EPS (10x). **(C)** *C. rudolphia* S-EPS network stained with Alcian Blue (10x). (**D**) SEM micrograph of *C. rudolphia* S-EPS. **(E)** Fluorescence microscopy showing PS-MPs (bright signal) retained within *C. rudolphia* S-EPS network (10x). **(F)** Purified S-EPS extracted from *C. rudolphia* recovered after ultrafiltration.

NMR spectra of S-EPS (D_2O, 70 °C; ES5; Fig. S7) corroborate the ATR-FTIR assignments. Resonances in 3.0–4.2 ppm (sugar-ring H-2-H-6) and 4.2–5.5 ppm (anomeric H-1) indicate multiple monosaccharide residues with mixed α/β configurations (Abeygunawardana et al., 2000; Gonzalez-Gil et al., 2015). Signals in 0.8–3.0 ppm arise from aliphatic protons of minor non-sugar constituents (*e.g.,* amino-acid side chains/lipids) (Seviour et al., 2010; Mishra et al., 2011; Gonzalez-Gil et al., 2015; Ledezma et al., 2016).

Electrostatic interactions were probed by zeta potential measurements (ζ; see Section 2.8). A common criterion is that $|\zeta| \geq 30$ mV indicates electrostatic stabilisation, whereas $|\zeta| < 30$ mV favours aggregation/flocculation. (Hanaor et al., 2012). PS-MPs showed $\zeta = -21.10 \pm 0.38$ mV (pH 7) (Table 1), indicating limited electrostatic stabilisation and a propensity to agglomerate. Together with the microscopy evidence of particle entrapment within S-EPS meshes, these data support charge neutralisation/bridging and physical enmeshment as dominant mechanisms for PS-MPs capture by *C. rudolphia* S-EPS.

3.3.2. *Exploring key factors in the bioflocculation process*

A comprehensive parametric evaluation was performed to confirm the suitability of *C. rudolphia* S-EPS for removing PS-MPs at a high load (2 g/L) under varying cation type and concentration, pH, salinity, S-EPS: PS-MPs ratio, and flocculation time. A high-load stress test was selected to delineate a conservative operating window where limitations are most visible. High particle counts increase collision frequency and tighten effect estimates, making bridging thresholds, pH/Fe^{3+} requirements, and ionic-strength limitations observable. The global effect ranking (Fig. S8) showed that cation type had the strongest influence, followed by pH and Fe^{3+} concentration; salinity and S-EPS dose showed comparable, intermediate effects, whereas time had the least impact. Negative coefficients in Fig. S8 denote conditions that improve flocculation relative to the reference, whereas positive coefficients denote impairment.

Table 1
Zeta potential (mV) of S-EPS, PS-MPs, and S-EPS/PS-MPs hetero-aggregates under different experimental conditions.

Cations effect (pH 7.0; 25 °C)	**Mg^{2+}**	**Ca^{2+}**	**Fe^{3+}**
PS-MPs	−6.49 ± 0.23	−15.50 ± 0.79****	−5.16 ± 0.28
S-EPS	−19.50 ± 0.72	−20.70 ± 1.05	−25.00 ± 1.00*
S-EPS/PS-MPs	−13.30 ± 0.75	−14.50 ± 0.74	−26.70 ± 0.98****
Fe^{3+} concentration effect (pH 3.5; 25 °C)	**0.03%**	**0.05%**	**0.3%**
S-EPS/PS-MPs	−19.30 ± 1.11	−16.40 ± 1.12	−6.48 ± 0.36****
pH effect (Fe^{3+} 0.05%; 25 °C)	**pH 3.0**	**pH 4.0**	
S-EPS/PS-MPs	−9.17 ± 0.09	−17.40 ± 0.85***	

pH effect (no added cation; 25 °C)	**3.0**	**3.5**	**4.0**	**6.0**	**7.0**
PS-MPs	−23.80 ± 1.30	−30.20 ± 1.71**	−19.00 ± 1.22*	−20.40 ± 0.88	−21.10 ± 0.38

Ratio effect (freshwater; pH 3.5; 25 °C; Fe^{3+} 0.05%)	**1:500**	**1:50**	**1:5**
S-EPS/PS-MPs	−19.00 ± 0.90	−14.70 ± 0.81**	−28.80 ± 0.54****

(*) denote statistical significance: *$p < 0.05$; **$p < 0.01$; ***$p < 0.001$; ****$p < 0.0001$. Data reported as mean ± SD (n = 3).

Cation type. Cations profoundly influence bioflocculation by mediating charge neutralisation and polymer-particle bridging (Lee et al., 2012; Zhu et al., 2012). Zeta potential data confirmed the presence of negative surfaces for PS-MPs and S-EPS and showed enhanced aggregation in the presence of multivalent ions (Table 1). For PS-MPs at pH 7 (no added cation), $\zeta = -21.10 \pm 0.38$ mV; addition of Ca^{2+} and Fe^{3+} shifted ζ to -15.50 ± 0.79 mV and -5.16 ± 0.28 mV, respectively (Table 1; Fig. S9A). These trends are consistent with stronger charge neutralisation and bridging by multivalent ions.

Cation concentration (Fe^{3+}). Flocculation efficiency displayed a non-monotonic dependence on Fe^{3+} (Sobeck and Higgins, 2002): 0.05 % (w/w, as $FeCl_3.6H_2O$) yielded the highest rates (Fig. S9B), whereas 0.03% was insufficient for optimal neutralisation and 0.3% reduced performance, likely due to charge reversal/over-dosing and sweep-floc/precipitation effects. Mixture ζ shifted from -19.30 ± 1.11 mV (0.03 %) to -16.40 ± 1.12 mV (0.05%) and -6.48 ± 0.36 mV (0.3%) (Table 1).

pH. Flocculation efficiency depended strongly on pH. *C. rudolphia* S-EPS showed maximal activity at acidic pH: pH 3.5 and pH 4.0 produced 82.31% and 72.16% efficiency, respectively (Fig. S9C). For S-EPS/PS-MPs mixtures at Fe^{3+} 0.05% (w/w), ζ was -9.17 ± 0.09 mV at pH 3.0 and -17.40 ± 0.85 mV at pH 4.0 (Table 1). For PS-MPs alone, ζ varied from -23.80 ± 1.30 mV (pH 3.0) to -30.20 ± 1.71 mV (pH 3.5) and -19.00 ± 1.22 mV (pH 4.0). Acidic conditions likely enhance protonation of S-EPS functional groups and modulate Fe^{3+} hydrolysis, favouring charge neutralisation/bridging.

Salinity. Ionic strength decreased flocculation efficiency (Fig. S9D). At pH 3.5 with Fe^{3+} 0.05%, mixture ζ shifted from -25.80 ± 0.10 mV (0 ‰) to -17.50 ± 0.74 mV (15 ‰) and -9.37 ± 0.51 mV (37 ‰) (Table 1), consistent with electrical double-layer compression and competition by Na^+, and potential $FeCl_3$ complexation, which weakens S-EPS-PS-MPs bridging.

S-EPS dose (S-EPS:PS-MPs). At 2 g/L PS-MPs, a higher polymer dose improved performance: 1:5 (w/w) > 1:50 > 1:500 (Fig. S9E). Mixtures reached -28.80 ± 0.54 mV at 1:5 (w/w) compared with -14.70 ± 0.81 (1:50) and -19.00 ± 0.90 (1:500) (Table 1; Fig. S9E), indicating that a bridging threshold must be exceeded for robust network formation. The 400 mg/L S-EPS condition delivered substantially higher rates, approaching the maximum observed (82.31%) and representing a 38% increase relative to the lowest S-EPS dose. For deployment, dose scales with particle load at the optimised mass ratio ($C_{S\text{-}EPS} = 0.2 \times C_{PS\text{-}MPs}$).

Flocculation time. Removal was evaluated at 30, 60, and 120 min (Fig. S9F). Maximum removal (*ca.* 80%) occurred at 60 min, with only marginal gains thereafter; accordingly, 60 min was adopted as the operational kinetic endpoint for optimisation.

Taken together, ζ-potential shifts (Table 1) and micrographs (Fig. 4) support a mechanism dominated by multivalent cation-mediated charge neutralisation/bridging and polymer enmeshment (Fig. 5), consistent with the observed dependencies on cation identity, pH, and ionic strength. Within the tested range, a practical operating window was identified: Fe^{3+} 0.05% (w/w), pH 3.5–4.0, low salinity, S-EPS:PS-MPs 1:5 (w/w), 60 min, achieving 80–82% removal at 2 g/L PS-MPs.

3.4. *S-EPS as a sustainable alternative for MPs mitigation*

The intended use is pretreatment of algal-cultivation intake waters, positioning cultivation-derived S-EPS as a low-additive, bio-based alternative compatible with standard coagulation/flocculation units. Conventional coagulants and flocculants, such as $FeCl_3$, aluminium-based salts, and synthetic polymers (*e.g.,* polyacrylamide), are widely used for MPs removal and can achieve efficiencies above 90% (Monira et al., 2021; Cui et al., 2024). However, these approaches typically generate metal-rich sludge, increase water salinity, and require tight pH control and subsequent sludge handling, which raise operational costs and environmental burdens (Alexander et al., 2012; Akinnawo et al., 2023; Cui et al., 2024).

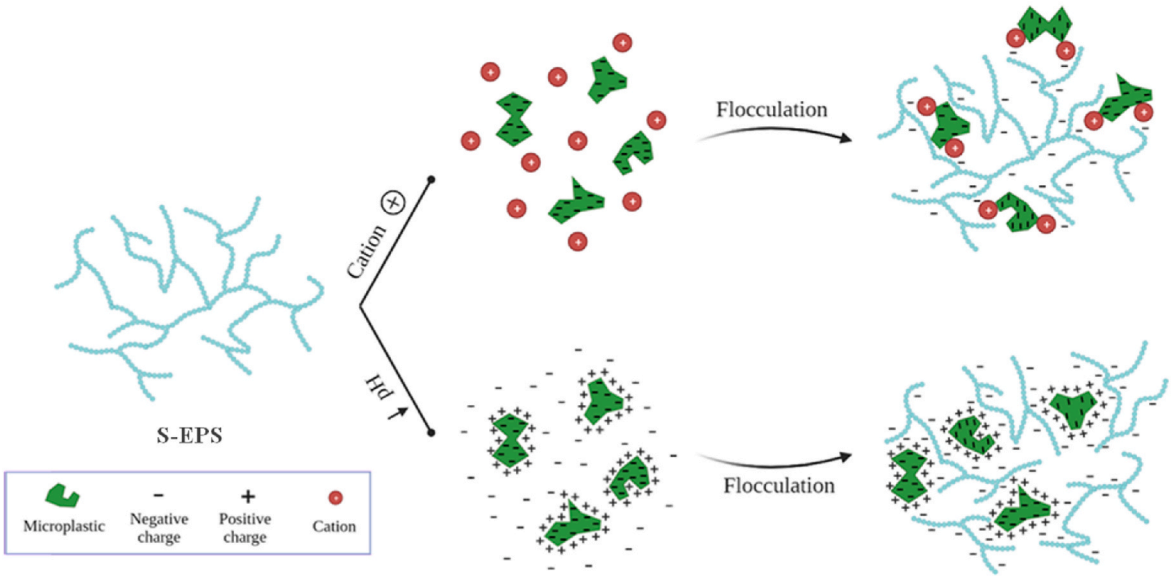

Fig. 5. Proposed mechanisms for PS-MPs flocculation by *C. rudolphia* S-EPS. Top: multivalent cations (*e.g.,* Fe^{3+}) bridge anionic S-EPS chains and negatively charged PS-MPs, enhancing aggregation. Bottom: acidic pH (3.5–4.0) protonates S-EPS functional groups and modulates particle charge, increasing charge neutralisation and polymer-particle binding. Together, these pathways promote hetero-aggregation and settling. Green shapes = PS-MPs; blue network = S-EPS; red circles = cations; "+/−" = surface charge.

Bioflocculants derived from microalgae offer a renewable, low-toxicity alternative. For example, *Scenedesmus* abundans achieved >84% total removal of PS, polymethyl methacrylate (PMMA), and polylactic acid (PLA) via EPS-mediated hetero-aggregation, with MPs pre-exposure enhancing EPS production (Cheng and Wang, 2022). EPS extracted after cationic surfactant pre-treatments, cetyltrimethylammonium bromide (CTAB) or dodecyltrimethylammonium bromide (DTAB), removed up to 86% of PE and PP, albeit at the cost of added chemicals/steps (Yaqoubnejad et al., 2023). An EPS-releasing *Chroococcidiopsis cubana* system reached 91% PS removal but required long exposure times (11 days) and high biomass densities (Das and Bal, 2025). *Chlorella vulgaris* EPS can also mediate PP/PET aggregation at high MPs loads (1000 mg/L), with EPS up-regulated by MPs exposure (Joelyna et al., 2024). Collectively, these routes often depend on long residence times, high cell densities, or chemical pre-treatments, which may limit practical deployment.

In contrast, the S-EPS naturally produced by *C. rudolphia* delivered up to 82% removal in a high-load stress test (2 g/L PS) within a compact operating window: Fe^{3+} 0.05% (w/w), pH 3.5–4.0, low salinity, S-EPS: PS-MPs of 1:5 (w/w), and 60 min contact time. For deployment, the required S-EPS dose scales with particle load: 50 μg/L PS requires 10 μg/L S-EPS, and 5 mg/L PS requires 1 mg/L S-EPS, assuming comparable water chemistry. At low particle counts, aggregation becomes collision-limited; therefore, longer contact times and gentle mixing are preferable to increasing polymer inventory. While peak removals with $FeCl_3$ alone can exceed 90%, S-EPS offers a bio-based option that can reduce added salinity and metal/sludge loads relative to purely chemical coagulation, at the cost of a narrower operating window at high salinity and the need for mild acidification. Consequently, the application is best suited to freshwater/low-salinity matrices or following ionic/pH pre-conditioning.

S-EPS are naturally derived, biodegradable polysaccharides. In jar tests, most of the added S-EPS co-sedimented with the flocs and were removed with the sludge, leaving only a small dissolved fraction. To minimise secondary impacts, operations should include post-treatment pH neutralisation, low Fe^{3+} inventories within regulatory norms, and compliant handling/disposal of MPs-rich sludge. A full appraisal of environmental safety will be addressed in follow-up work, including biodegradation (BOD/COD decay) and ecotoxicity assays under representative matrices.

4. Conclusion

Response surface modelling identified the biomass-to-medium ratio, time, and nitrogen as the main drivers of S-EPS synthesis by *C. rudolphia* (BEA 0786B); exposure to PS-MPs (50 μg/L; 5 mg/L) increased S-EPS production without broadly compromising biomass, enabling cost-lean production coupled to reuse as a low-additive pretreatment. Under a high-load benchmark (2 g/L PS-MPs), S-EPS achieved 80–82% removal within a compact window (Fe^{3+} 0.05% w/w; pH 3.5–4.0; low salinity; S-EPS:PS-MPs 1:5 w/w; 60 min), consistent with multivalent-cation–mediated charge neutralisation/bridging and polymer enmeshment. Effectiveness is matrix-dependent (reduces at high ionic strength); the approach is compatible with standard coagulation/flocculation units and offers lower added metal levels and reduced sludge relative to mineral coagulants. Future work will quantify biodegradation/ecotoxicity and validate pilot/continuous-flow performance across water chemistries and polymer types.

CRediT authorship contribution statement

Filipa Rodrigues: Writing – review & editing, Writing – original draft, Visualization, Formal analysis, Data curation. **Ivana Mendonça:** Writing – review & editing, Writing – original draft, Visualization, Formal analysis. **Marisa Faria:** Writing – review & editing, Validation, Methodology, Investigation, Formal analysis, Conceptualization. **Ricardo Gomes:** Writing – original draft, Investigation, Data curation. **Juan L. Gómez Pinchetti:** Writing – review & editing, Supervision, Resources, Project administration, Funding acquisition. **Artur Ferreira:** Writing – review & editing, Supervision, Resources, Project administration, Funding acquisition. **Nereida Cordeiro:** Supervision, Resources, Project administration, Funding acquisition, Conceptualization.

Ethics approval

Not applicable.

Declaration of generative AI in writing

During manuscript drafting, the authors used ChatGPT solely for language polishing. The authors reviewed and edited the text and are responsible for all content. No generative AI was used to create or alter figures, images, or artwork.

Funding

This work was supported by the European Territorial Cooperation Programme Interreg MAC 2021–2027 through project CALYPSO (1/MAC/1/1.1/0088) and also funded by national funds through FCT - Fundação para a Ciência e a Tecnologia, I.P., and by the European Commission's Recovery and Resilience Facility, within the scope of UID/04423/2025 (https://doi.org/10.54499/UID/04423/2025), UID/PRR/04423/2025 (https://doi.org/10.54499/UID/PRR/04423/2025), and LA/P/0101/2020 (https://doi.org/10.54499/LA/P/0101/2020). Filipa Rodrigues (2024.01262.BD), Ivana Mendonça (2023.04389.BD), and Marisa Faria (2020.6615.BD) were supported by FCT doctoral grants. The funders had no role in study design, data collection, analysis, interpretation, or the decision to submit the article.

Declaration of competing interest

The authors declare that they have no known competing financial interests or personal relationships that could have appeared to influence the work reported in this paper.

Appendix A. Supplementary data

Supplementary data to this article can be found online at https://doi.org/10.1016/j.chemosphere.2025.144759.

Data availability

Data will be made available on request.

References

Abeygunawardana, C., Williams, T.C., Sumner, J.S., et al., 2000. Development and validation of an NMR-based identity assay for bacterial polysaccharides. Anal. Biochem. 279, 226–240.
Agunbiade, M., Oladipo, B., Ademakinwa, A.N., et al., 2022. Bioflocculant produced by *Bacillus velezensis* and its potential application in brewery wastewater treatment. Sci. Rep. 12, 1–12.
Ahmed, Z., Mehmood, T., Ferheen, I., Noori, A.W., Almansouri, M., Waseem, M., 2023. Optimisation of exopolysaccharide produced by *L. kefiranofaciens* ZW3 using response surface methodology. Int. J. Food Prop. 26, 2285–2293.
Akinnawo, S.O., Ayadi, P.O., Oliwalope, M.T., 2023. Chemical coagulation and biological techniques for wastewater treatment. Sciendo 34, 14–21.
Alexander, J.T., Hai, F.I., Al-aboud, T.M., 2012. Chemical coagulation-based processes for trace organic contaminant removal: current state and future potential. Environ. Manag. 111, 195–207.
Asgher, M., Urooj, Y., Qamar, S.A., Khalid, N., 2020. Improved exopolysaccharide production from *Bacillus licheniformis* MS3: optimisation and structural/functional characterisation. Int. J. Biol. Macromol. 151, 984–992.
Barnes, D.K.A., Galgani, F., Thompson, R.C., et al., 2009. Accumulation and fragmentation of plastic debris in global environments. Philos. Trans. R. Soc. B 364, 1985–1998.
Borah, D., Rethinam, G., Gopalakrishnan, S., et al., 2020. Ozone enhanced production of potentially useful exopolymers from the cyanobacterium *Nostoc muscorum*. Polym. Test. 84, 106385.
Camacho-Chab, J.C., Lango-Reynoso, F., Castañeda-Chávez, M. del R., et al., 2016. Implications of extracellular polymeric substance matrices of microbial habitats associated with coastal aquaculture systems. Water 8, 1–21.
Cheng, Y., Wang, H., 2022. Highly effective removal of microplastics by microalgae *Scenedesmus abundans*. Chem. Eng. J. 435, 135079.
Cole, M., Lindeque, P., Fileman, E., et al., 2015. The impact of polystyrene microplastics on feeding, function and fecundity in the marine Copepod *Calanus helgolandicus*. Environ. Sci. Technol. 2, 1130–1137.
Costa, O.Y.A., Raaijmakers, J.M., Kuramae, E.E., 2018. Microbial extracellular polymeric substances: ecological function and impact on soil aggregation. Front. Microbiol. 9, 1–14.
Cruz, D., Vasconcelos, V., Pierre, G., Michaud, P., Delattre, C., 2020. Exopolysaccharides from cyanobacteria: strategies for bioprocess development. Appl. Sci. 10, 3763.
Cui, B., Rong, H., Tian, T., et al., 2024. Chemical methods to remove microplastics from wastewater: a review. Environ. Res. 204, 118416.
Cunha, C., Faria, M., Nogueira, N., Ferreira, A., Cordeiro, N., 2019. Marine *vs* freshwater microalgae exopolymers as biosolutions to microplastics pollution. Environ. Pollut. 249, 372–380.
Cunha, C., Lopes, J., Paulo, J., Faria, M., Kaufmann, M., Nogueira, N., Ferreira, A., Cordeiro, N., 2020a. The effect of microplastics pollution in microalgal biomass production: a biochemical study. Water Res. 186, 116370.
Cunha, C., Silva, L., Paulo, J., et al., 2020b. Microalgal-based biopolymer for nano- and microplastic removal: a possible biosolution for wastewater treatment. Environ. Pollut. 263, 114385.
Das, P., Bal, M., 2025. Modeling and optimization study for microplastic removal from aquatic medium using *Chroococcidiopsis* species. Chem. Eng. Sci. 304, 121085.
Demir-Yilmaz, I., Yakovenko, N., Roux, C., et al., 2022. The role of microplastics in microalgae cells aggregation: a study at the molecular scale using atomic force microscopy. Sci. Total Environ. 832, 155036.
Ding, R., Tong, L., Zhang, W., 2021. Microplastics in freshwater environments: sources, fates and toxicity. Water Air Soil Pollut. 232.
Ebrahimi, P., Abbasi, S., Pashaei, R., Bogusz, A., Oleszczuk, P., 2022. Investigating impact of physicochemical properties of microplastics on human health: a short bibliometric analysis and review. Chemosphere 289, 133146.
Elizalde-Velázquez, G.A., Gómez-Oliván, L.M., 2021. Microplastics in aquatic environments: a review on occurrence, distribution, toxic effects, and implications for human health. Sci. Total Environ. 780, 146551.
Esmaeili Nasrabadi, A., Kabirinia, F., Bonyadi, Z., 2025a. Assessment of microplastic release from facial and body scrubs in aquatic ecosystems. Appl. Water Sci. 15, 19.
Esmaeili Nasrabadi, A., Babaei, N., Bonyadi, Z., 2025b. Effect of ozonation on the morphological characteristics and adsorption behavior of polystyrene microplastics in aqueous environments. Appl. Water Sci. 15, 90.
Faria, M., Cunha, C., Gomes, M., et al., 2022. Bacterial cellulose biopolymers: the sustainable solution to water-polluting microplastics. Water Res. 222, 118952.
Feng, C., Lotti, T., Canziani, R., et al., 2021. Extracellular biopolymers recovered as raw biomaterials from waste granular sludge and potential applications: a critical review. Sci. Total Environ. 753, 142051.
Franco-Morgado, M., Amador-Espejo, G.G., Pérez-Cortés, M., Gutiérrez-Uribe, J.A., 2023. Microalgae and Cyanobacteria polysaccharides: important link for nutrient recycling and revalorization of agro-industrial wastewater. Appl. Food Res. 3, 100296.
Gonzalez-Gil, G., Thomas, L., Emwas, A.H., et al., 2015. NMR and MALDI-TOF MS based characterization of exopolysaccharides in anaerobic microbial aggregates from full-scale reactors. Sci. Rep. 5, 14316.
Hanaor, D., Michelazzi, M., Leonelli, C., Sorrell, C.C., 2012. The effects of carboxylic acids on the aqueous dispersion and electrophoretic deposition of ZrO_2. J. Eur. Ceram. Soc. 32, 235–244.
Jiménez-Skrzypek, G., Hernández-Sánchez, C., Ortega-Zamora, C., González-Sálamo, J., González-Curbelo, M.Á., Hernández-Borges, J., 2021. Microplastic-adsorbed organic contaminants: analytical methods and occurrence. TrAC, Trends Anal. Chem. 136, 116186.
Joelyna, F.A., Hadiyanto, Khroironi, A., et al., 2024. The utilization of exopolysaccharide (EPS) from microalgae *Chlorella vulgaris* in microplastic removal. IOP Conf. Ser. Earth Environ. Sci. 1414, 012017.
Jung, P., Sommer, V., Karsten, U., Lakatos, M., 2022. Salty twins: salt-tolerance of terrestrial *Cyanocohniella* strains (Cyanobacteria) and description of *C. rudolphia* sp. Nov. point towards a marine origin of the genus and terrestrial long distance dispersal patterns. Microorganisms 10, 968.
Kaplan Can, H., Gurbuz, F., Odabaşı, M., 2019. Partial characterisation of cyanobacterial extracellular polymeric substances for aquatic ecosystems. Aquat. Ecol. 53, 431–440.
Ledezma, O., Méndez, H., Manjarrez, L., et al., 2016. Characterization of extracellular polymeric substances (EPS) produced by marine *Micromonospora sp*. J. Chem. Pharmaceut. Res. 8, 442–451.
Lee, B.J., Schlautman, M.A., Toorman, E., Fettweis, M., 2012. Competition between kaolinite flocculation and stabilisation in divalent cation solutions dosed with anionic polyacrylamides. Water Res. 46, 5696–5706.
Li, S., Wang, P., Zhang, C., et al., 2020. Influence of polystyrene microplastics on the growth, photosynthetic efficiency and aggregation of freshwater microalgae *Chlamydomonas reinhardtii*. Sci. Total Environ. 714, 136767.
Liberton, M., Biswas, S., Pakrasi, H.B., 2022. Photosynthetic modulation during the diurnal cycle in a unicellular diazotrophic cyanobacterium grown under nitrogen-replete and nitrogen-fixing conditions. Sci. Rep. 12, 1–12.
Mehra, A., Jutur, P.P., 2022. Application of response surface methodology (RSM) for optimising biomass production in *Nannochloropsis oculata* UTEX 2164. J. Appl. Phycol. 34, 1893–1907.
Mendonça, I., Cunha, C., Kaufmann, M., et al., 2023a. Microplastics reduce microalgal biomass by decreasing single-cell weight: the barrier towards implementation at scale. Sci. Total Environ. 877, 162950.
Mendonça, I., Faria, M., Rodrigues, F., Cordeiro, N., 2024. Microalgal-based industry vs. microplastic pollution: current knowledge and future perspectives. Sci. Total Environ. 909, 168414.
Mendonça, I., Sousa, J., Cunha, C., et al., 2023b. Solving urban water microplastics with bacterial cellulose hydrogels: leveraging predictive computational models. Chemosphere 314, 137719.
Mishra, A., Kavita, K., Jha, B., 2011. Characterization of extracellular polymeric substances produced by micro-algae *Dunaliella salina*. Carbohydr. Polym. 83, 852–857.

Monira, S., Brhuiyan, M.A., Haque, N., et al., 2021. Assess the performance of chemical coagulation process for microplastics removal from stormwater. Process. Saf. Environ. Prot. 155, 11–16.
Nobrega, V., Faria, M., Quintana, A., et al., 2019. From a basic microalga and an acetic acid bacterium cellulose producer to a living symbiotic biofilm. Materials 12, 2275.
Revel, M., Châtel, A., Mouneyrac, C., 2018. Micro(nano)plastics: a threat to human health? Curr. Opin. Environ. Sci. Health 1, 17–23.
Rist, S., Carney Almroth, B., Hartmann, N.B., Karlsson, T.M., 2018. A critical perspective on early communications concerning human health aspects of microplastics. Sci. Total Environ. 626, 720–726.
Rodrigues, F., Mendonça, I., Faria, M., et al., 2025. Development, Optimisation and Validation of an Alcian Blue-based Assay for soluble- Extracellular Polymeric Substances (S-EPS) Quantification submitted for publication.
Rodrigues, F., Mendonça, I., Faria, M., Gomes, R., Pinchetti, J.L.G., Ferreira, A., Cordeiro, N., 2024a. Response surface methodology applied to cyanobacterial EPS production: steps and statistical validations. Processes 12, 1733.
Rodrigues, F., Faria, M., Mendonça, I., Sousa, E., Ferreira, A., Cordeiro, N., 2024b. Efficacy of bacterial cellulose hydrogel in microfiber removal from contaminated waters: a sustainable approach to wastewater treatment. Sci. Total Environ. 919, 170846.
Sarijan, S., Azman, S., Said, M.I.M., Jamal, M.H., 2021. Microplastics in freshwater ecosystems: a recent review of occurrence, analysis, potential impacts, and research needs. Environ. Sci. Pollut. Res. 28, 1341–1356.
Seviour, T., Lambert, L.K., Pijuan, M., et al., 2010. Structural determination of a key exopolysaccharide in mixed culture aerobic sludge granules using NMR spectroscopy. Environ. Sci. Technol. 44, 8964–8970.
Sheikh, T., Hamid, B., Baba, Z., et al., 2022. Extracellular polymeric substances in psychrophilic cyanobacteria: a potential bioflocculant and carbon sink to mitigate cold stress. Biocatal. Agric. Biotechnol. 42, 102375.
Siddharth, T., Sridhar, P., Vinila, V., Tyagi, R.D., 2021. Environmental applications of microbial extracellular polymeric substance (EPS): a review. J. Environ. Manag. 287, 112307.
Sobeck, D.C., Higgins, M.J., 2002. Examination of three theories for mechanisms of cation-induced bioflocculation. Water Res. 36, 527–538.
Tawila, Z.M.A., Ismail, S., Dadrasnia, A., Usman, M.M., 2018. Production and characterisation of a bioflocculant produced by *Bacillus salmalaya* 139SI-7 and its applications in wastewater treatment. Molecules 23, 2689.
Tiwari, O.N., Khangembam, R., Shamjetshabam, M., et al., 2015. Characterisation and optimisation of bioflocculant exopolysaccharide production by Cyanobacteria *Nostoc* sp. BTA97 and *Anabaena* sp. BTA990 in culture conditions. Appl. Biochem. Biotechnol. 176, 1950–1963.
Trabelsi, L., Ben Ouada, H., Bacha, H., Ghoul, M., 2009. Combined effect of temperature and light intensity on growth and extracellular polymeric substance production by the cyanobacterium *Arthrospira platensis*. J. Appl. Phycol. 21, 405–412.
Wagner, M., Lambert, S. (Eds.), 2018. Freshwater Microplastics. the Handbook of Environmental Chemistry, 58. Springer.
Wang, Y., Zhang, D., Zhang, M., et al., 2019. Effects of ingested polystyrene microplastics on brine shrimp. Artemia parthenogenetica. Environ. Pollut. 244, 715–722.
Xiao, R., Zheng, Y., 2016. Overview of microalgal extracellular polymeric substances (EPS) and their applications. Biotechnol. Adv. 34, 1225–1244.
Xie, X., Deng, T., Duan, J., et al., 2020. Exposure to polystyrene microplastics causes reproductive toxicity through oxidative stress and activation of the p38 MAPK signaling pathway. Ecotoxicol. Environ. Saf. 190, 110133.
Xu, H., Yu, G., Jiang, H., 2013. Investigation on extracellular polymeric substances from mucilaginous cyanobacterial blooms in eutrophic freshwater lakes. Chemosphere 93, 75–81.
Yaqoubnejad, P., Abdolalian, S., Taghavijeloudar, M., et al., 2023. Microplastics removal from water bodies by extracellular polymeric substances (EPS) extracted from microalgae through surfactant pre-treatment. In: Proceedings of the 7th International Conference on Researches in Science & Engineering and the 4th International Congress on Civil, Architecture and Urbanism in Asia.
Yuan, Z., Nag, R., Cummins, E., 2022. Human health concerns regarding microplastics in the aquatic environment-from marine to food systems. Sci. Total Environ., 153730
Zhao, B., Rehati, P., Yang, Z., et al., 2024. The potential toxicity of microplastics on human health. Sci. Total Environ. 912, 168946.
Zhao, D., Liu, L., Jiang, J., et al., 2020. The response surface optimisation of exopolysaccharide produced by *Weissella confusa* XG-3 and its rheological property. Prep. Biochem. Biotechnol. 50, 1014–1022.
Zhu, C., Chen, C., Zhao, L., et al., 2012. Bioflocculant produced by *Chlamydomonas reinhardtii*. J. Appl. Phycol. 24, 1245–1251.